Biointerphases
A Journal of Biomaterials and Biological Interfaces

# Detection of gold cysteine thiolate complexes on gold nanoparticles with time-of-flight secondary ion mass spectrometry

Cite as: Biointerphases **16**, 021005 (2021); https://doi.org/10.1116/6.0000910
Submitted: 04 January 2021 . Accepted: 17 March 2021 . Published Online: 02 April 2021

Heng-Yong Nie, Elena Romanovskaia, Valentin Romanovski, Jonas Hedberg, and Yolanda S. Hedberg

Biointerphases
A Journal of Biomaterials and Biological Interfaces

ARTICLE

avs.scitation.org/journal/bip

# Detection of gold cysteine thiolate complexes on gold nanoparticles with time-of-flight secondary ion mass spectrometry

Cite as: Biointerphases 16, 021005 (2021); doi: 10.1116/6.0000910
Submitted: 4 January 2021 · Accepted: 17 March 2021 ·
Published Online: 2 April 2021



Heng-Yong Nie,[1,2,a)] Elena Romanovskaia,[3,4] Valentin Romanovski,[5,6] Jonas Hedberg,[1,3] and Yolanda S. Hedberg[1,3,7,b)]

## AFFILIATIONS

[1]Surface Science Western, The University of Western Ontario, 999 Collip Circle, London, Ontario N6G 0J3, Canada
[2]Department of Physics and Astronomy, The University of Western Ontario, London, Ontario N6A 3K7, Canada
[3]Department of Chemistry, Division of Surface and Corrosion Science, KTH Royal Institute of Technology, SE-10044 Stockholm, Sweden
[4]Department of Chemistry, Technology of Electrochemical Production and Electronic Engineering Materials, Belarusian State Technological University, Sverdlova st., 13, 220006 Minsk, Belarus
[5]Institute of General and Inorganic Chemistry, National Academy of Sciences of Belarus, Surganova st., 9/1, 220072 Minsk, Belarus
[6]Science and Research Centre of Functional Nano-Ceramics, National University of Science and Technology "MISIS", Lenin av., 4, 119049 Moscow, Russia
[7]Department of Chemistry, The University of Western Ontario, London, Ontario N6A 5B7, Canada

[a)]**Electronic mail:** hnie@uwo.ca
[b)]**Electronic mail:** yhedberg@uwo.ca

## ABSTRACT

Gold (Au) nanoparticles (NPs) are widely used in nanomedical applications as a carrier for molecules designed for different functionalities. Previous findings suggested that biological molecules, including amino acids, could contribute to the dissolution of Au NPs in physiological environments and that this phenomenon was size-dependent. We, therefore, investigated the interactions of L-cysteine with 5-nm Au NPs by means of time-of-flight secondary ion mass spectrometry (ToF-SIMS). This was achieved by loading Au NPs on a clean aluminum (Al) foil and immersing it in an aqueous solution containing L-cysteine. Upon rinsing off the excessive cysteine molecules, ToF-SIMS confirmed the formation of gold cysteine thiolate via the detection of not only the Au–S bond but also the hydrogenated gold cysteine thiolate molecular ion. The presence of NaCl or a 2-(N-morpholino)ethanesulfonic acid buffer disabled the detection of Au NPs on the Al foil. The detection of larger (50-nm) Au NPs was possible but resulted in weaker cysteine and gold signals, and no detected gold cysteine thiolate signals. Nano-gold specific adsorption of L-cysteine was also demonstrated by cyclic voltammetry using paraffine-impregnated graphite electrodes with deposited Au NPs. We demonstrate that the superior chemical selectivity and surface sensitivity of ToF-SIMS, via detection of elemental and molecular species, provide a unique ability to identify the adsorption of cysteine and formation of gold–cysteine bonds on Au NPs.



## I. INTRODUCTION

Gold nanoparticles (Au NPs) are widely considered for different nanomedical applications, including tumor targeting, drug delivery, imaging, and molecular sensing.[1–6] Their fate in the human body, including changing surface chemistries, degradation kinetics, toxicity, and their clearance from the body, is complex and remains a hindering factor for successful clinical use.[2,7] All considered Au NPs are functionalized (surface-coated) with a

capping agent to hinder their aggregation and enable their dispersion in aqueous solutions. For example, citrate-coated Au NPs are relatively stable in a citrate buffer but can be assumed to interact with other biomolecules once injected in the human body.[8] Studies using physiologically based pharmacokinetic models suggested that relatively inert NPs, such as Au NPs, might still dissolve to some extent over time in the human body.[9] We have earlier shown that citrate-coated Au NPs dissolve up to 14% after one week of incubation in cell medium at physiological *p*H and 37 °C, when triggered by stimulated macrophages. This effect is size-dependent, that is, largest for 5 nm Au NPs (14% dissolution for 5 nm and 0.6% for 50 nm Au NPs under these conditions).[10] This nano-specific dissolution could not be explained by the difference in the specific surface area alone and was only seen under relatively aggressive conditions and only in the presence of biomolecules.[10] The smaller size can influence dissolution and surface reactions in several ways: by changing the diffusion layer thickness, by a larger surface to bulk atom ratio of smaller-sized nanoparticles, and by changing lattice parameters and surface energies affecting dissolution equilibrium constants.[11] Most of these nano-specific effects dominate only well below 10 nm.[12] NPs below 20 nm cannot easily be separated from solution[10,13,14] and it is hence difficult to study dynamic adsorption or binding processes. Biomolecules have been seen to play an important role for the nano-specific dissolution of Au NPs.[10] We therefore studied L-cysteine, which is an important amino acid with a thiol side chain known to interact with gold and to easily displace other ligands from Au NPs.[15]

The interaction between gold and cysteine has been explored with molecular dynamics simulation,[16] x-ray photoelectron spectroscopy,[17] Raman spectroscopy, and infrared absorption spectroscopy.[18] However, the latter methods require a relatively large amount of Au NPs (milligrams or more).

Time-of-flight secondary ion mass spectrometry (ToF-SIMS)[19] is an extremely surface sensitive technique, probing the topmost 1–3 nm of a surface. ToF-SIMS has been widely used to investigate self-assembled monolayers (SAMs) of alkanethiols on Au.[20,21] By contrast, mass spectrometry studies on the interaction of gold and the thiol group of biomolecules are rather scarce.[22] A previous ToF-SIMS study on examining cysteine reported the detection of hydrogenated and dehydrogenated molecular ions.[23] To our best knowledge, there are no ToF-SIMS studies on the interaction between cysteine and gold or Au NPs. Therefore, we conducted an investigation on a simplified model system involving only a L-cysteine solution and Au NPs deposited on an aluminum (Al) foil using ToF-SIMS in order to further understand the interaction between cysteine and Au NPs in the physiological environment containing L-cysteine and other biomolecules able to interact with Au NPs. The surface sensitive ToF-SIMS, with superior chemical selectivity, provides a powerful approach to explore surface/interface chemistry[19,24–28] of cysteine monolayers adsorbed or even bonded to Au NPs. The ToF-SIMS results were compared with electrochemical measurements.

The aim of this study was to (*i*) elaborate a ToF-SIMS method able to detect interactions between Au NPs and cysteine, and to (*ii*) identify the type of these interactions for 5-nm Au NPs, and (*iii*) evaluate if the method can also be used for the larger-sized 50-nm Au NPs.

## II. EXPERIMENT

### A. Materials and chemicals

Aqueous suspensions of citrate-coated Au NPs, stabilized in citrate buffer, sized 5 and 50 nm were purchased from Millipore Sigma (Canada and Sweden, product Nos. 741949 and 742007). According to the supplier, the suspensions contained $5.5 \times 10^{13}$ particles/ml for the 5-nm and $3.5 \times 10^{10}$ particles/ml for the 50-nm Au NPs, corresponding to a mass concentration (assuming a gold density of 19.23 g/cm$^3$) of 69.5 $\mu$g/ml for the 5-nm and 44.3 $\mu$g/ml for the 50-nm Au NPs.

The solvent for all experiments was ultrapure water (resistivity of 18.2 MΩcm, Millipore Sigma, Canada and Sweden).

L-cysteine (≥98%, product No. C7352) and 2-(N-morpholino) ethanesulfonicacid (MES) buffer were obtained from Millipore Sigma (Canada and Sweden). Sodium chloride (analytical grade) and ultrapure nitric acid (67%) were obtained from VWR (Sweden).

### B. Transmission and scanning electron microscopy

A transmission electron microscopy (TEM) JEOL 2100 instrument (Jeol Ltd., Japan) equipped with an x-ray energy dispersive spectrometer was used to image the 5-nm Au NPs, dropped from their suspension on the TEM grid, followed by drying.

A scanning electron microscope (JEOL F7600, Jeol Ltd., Japan) using 15 kV accelerating voltage and the secondary electron detection mode was used to image the 50-nm Au NPs, dispersed (nondiluted, $\mu$l-drop) on carbon tape, followed by drying.

The IMAGEJ software (version 1.52v) was used to evaluate the size of 196 particles (5-nm Au NPs) and 175 particles (50-nm Au NPs) from those images to obtain quantitative size distribution information. The cumulative size distribution curves were plotted in Origin 2016 and differentiated. The resulting size distribution was smoothed using the adjacent-averaging method with ten points of window.

### C. Electrochemical measurements

A paraffine-impregnated graphite electrode (PIGE), known to have a low background current,[29] was used as the working electrode. An Ag/AgCl 3M KCl electrode (Ametek, US) was used as a reference electrode and a platinum wire (Millipore Sigma, Sweden) was used as counter electrode in a home-built cell inserting the PIGE from the bottom and the reference and counter electrode from the top into an electrolyte volume of 3 ml. Prior to each measurement, the PIGE was rinsed with ultrapure water, ground, and rinsed again with ultrapure water. The Au NP suspension was vortexed for 10 s after which a defined volume (8 $\mu$l for 5-nm and 12.6 $\mu$l for 50-nm Au NPs) was pipetted on the PIGE corresponding to a mass of Au NPs of $5.56 \times 10^{-4}$ mg in each case, followed by 1 h drying at room temperature. All cyclic voltametric measurements started at open-circuit potential (OCP, first measured for 5 min) and scanned anodically (to more positive potentials) at a scan rate of 0.5 mV/s to 1 V versus Ag/AgCl (3M KCl), after which the scan was reversed to OCP. All measurements were conducted at aerated conditions and room temperature (22 ± 2 °C) without any stirring. A 5 g/l NaCl in 5 mM MES buffer at *p*H 7.4 (adjusted by

nitric acid) was used as a background control electrolyte without Au NPs, with 5-nm, and with 50-nm Au NPs. 0.5 mM L-cysteine and 5 g/l NaCl in 5 mM MES buffer (*p*H 7.4) was used without Au NPs, with 5-nm and with 50-nm Au NPs. In addition, the 5-nm Au NPs were also investigated in electrolytes containing 0.05, 0.1, 0.5, and 5 mM L-cysteine in 5 g/l NaCl and 5 mM MES buffer (*p*H 7.4).

### D. ToF-SIMS

A clean Al foil was used to deposit the citrate-coated 5-nm Au NPs with a pipette from the Au NP suspension, followed by drying at room temperature. The Au NPs-loaded Al foil was rinsed with ultrapure water for at least 20 s to investigate whether Au could be detected by ToF-SIMS. Another two pieces of Au NPs-loaded Al foils were immersed in a 5 mM L-cysteine solution for 1 day at room temperature. One was taken out from the solution and naturally dried and the other was rinsed with ultrapure water. The 5 mM L-cysteine solution had a *p*H of 5.3. Measurements in lower concentrated L-cysteine solution or after immersion in solutions containing MES buffer and NaCl were insufficient for the detection of the Au NPs, which is the reason why 5 mM L-cysteine was chosen. The same method was also used for the larger-sized (50-nm) Au NPs. The molecular formula of L-cysteine, $SC_3H_7NO_2$, is shown in Fig. 1(a). Any interaction between cysteine and gold is expected to form gold cysteine thiolate, $AuSC_3H_6NO_2$, as shown in Fig. 1(b).

ToF-SIMS (TOF-SIMS IV, ION-TOF GmbH, Germany) was used to study the interaction between L-cysteine and the Au NPs. In ToF-SIMS, the sample surface was bombarded with a pulsed (~1 ns) 25 keV $Bi_3^+$ primary ion beam for generation of ions from the surface. These secondary ions were extracted with an electric field and their times of flight in a reflectron type of tube were measured to construct a spectrum of secondary ion mass by converting the flight time to a mass/charge (*m*/*z*) ratio via known species such as hydrogen, carbon, and hydrocarbons. A low energy electron beam was then flooded over the sample for charge compensation, which completed the 100-$\mu$s cycle of one shot of the primary ion. The base pressure of the analysis chamber of the instrument was about $10^{-7}$ mbar. The secondary ion mass spectra were collected at $128 \times 128$ pixels over the rastered area with one shot of pulsed primary ion beam per pixel. The ion mass spectra presented in this study were normalized to the total ion intensity because spectra collected from areas with different sizes were compared. Negative ion mass spectra were calibrated using $CH^-$, $C_2H^-$, and $C_4H^-$. Positive ion mass spectra were calibrated using $CH_3^+$, $C_4H_7^+$, and $C_6H_9^+$. The mass resolution for $CH^-$, $C_4H^-$, $CH_3^+$, and $C_4H_7^+$ was 3000, 4500, 3800, and 5300, respectively. An image of an ion was obtained by mapping the intensity of the ion against the pixels. The resolution of ion image was on the order of a couple of micrometers.

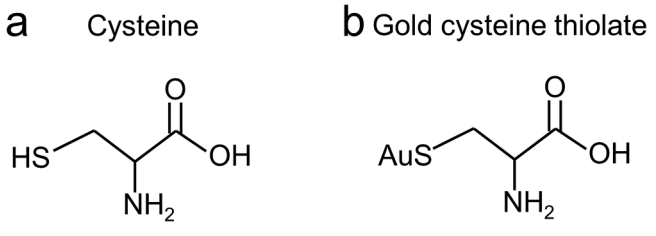


**FIG. 1.** Chemical formula of L-cysteine (a) and a possible interaction between cysteine and gold to form gold cysteine thiolate (b).

## III. RESULTS AND DISCUSSION

### A. Particle size characterization

The experimental design of the ToF-SIMS and electrochemical studies involved the deposition of the gold suspension on a substrate (PIGE or Al foil) and drying in air at room temperature, prior to exposure to L-cysteine-containing solutions. The same approach was used to study the size distribution of the particles by means of TEM and SEM. Figure 2 shows the size distribution of the 5 and 50-nm Au NPs. The mean values of the size distribution are exactly 5 and 50 nm, which means a specific surface area difference of 100. It can also be deduced that there is a larger agglomeration tendency for the 5-nm Au NPs as compared to 50-nm Au NPs, which is in agreement with earlier observations on a different batch of similar suspensions.[10] For the substrate-deposition approach used in our electrochemical and ToF-SIMS investigations, we could hence expect a possible greater adherence of the 5-nm Au NPs and a 100× larger surface area for the same deposited mass compared with the 50-nm Au NPs.

### B. Electrochemical detection of gold–cysteine interactions

The PIGE working electrode and the chosen MES buffer and NaCl electrolyte showed a low background current and no peaks [Fig. 3(a)]. Once the PIGE was loaded with Au NPs, the signal differed significantly with a higher background current anodic to about 0.4 V (versus Ag/AgCl 3M KCl), possibly some peaks at 0.6–1.0 V, of which some seemed to be very sharp. The peak position[30,31] and the sharpness of the peaks (due to mass limitation of few activated particles[32]) are indicative of gold oxidation of a small fraction of the loaded Au NPs. Indeed, the total charge of the peaks corresponded to less than 0.001% of the deposited gold mass suggesting negligible gold oxidation under these experimental conditions. The background current increased in the presence of 0.5 mM L-cysteine, probably due to some oxidation of cysteine on the PIGE. With Au NPs loaded, the relatively broad cysteine peak, located at around 0.4–0.8 V, increased significantly, however, as expected, much more significantly for the 5-nm Au NPs than the 50-nm Au NPs. These observations on a cysteine oxidation peak amplified on gold agree with those found on nanoporous gold electrodes when compared to glassy carbon electrodes.[31] It has been suggested[31] that the broadness of the cysteine oxidation peak origins from a two-step oxidation [Eqs. (1) and (2)], where ads denotes adsorbed, CySH denotes cysteine, and $CySO_3^-$ denotes cysteic acid,

$$CySH_{ads} \rightarrow CyS\cdot_{ads} + H^+ + e^-, \quad (1)$$

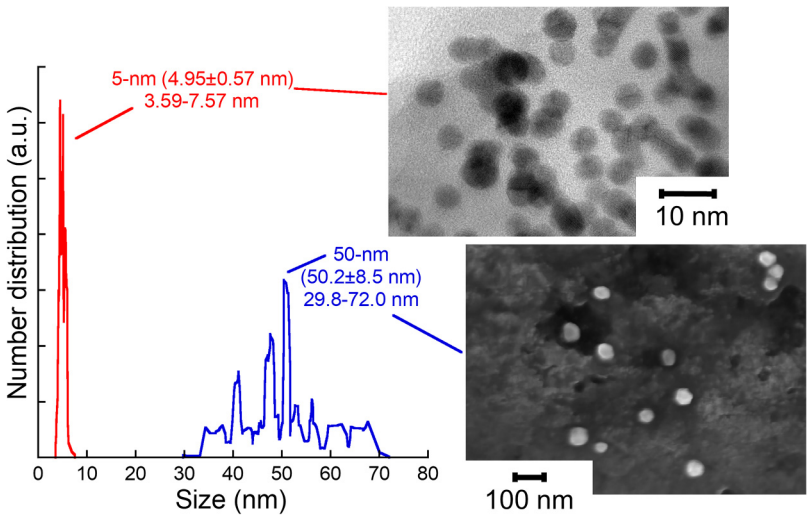


**FIG. 2.** Number size distribution based on TEM images (5-nm Au NPs) and SEM images (50-nm Au NPs). The mean and standard deviation, as well as the minimum and maximum size found in these images, are based on in total 196 and 175 evaluated particles for the 5-nm and 50-nm Au NPs, respectively.

$$CyS\cdot_{ads} + H_2O \rightarrow CySO_3^- + 5e^- + 6H^+. \quad (2)$$

It should be noted that gold and cysteine oxidation peaks overlap and may influence each other. This will be investigated in future studies. Different L-cysteine concentrations were also studied for the same mass ($5.56 \times 10^{-4}$ mg) of deposited 5-nm Au NPs [Figs. 3(c)–3(d)]. The cysteine oxidation peak was increasing linearly with increasing solution concentration, except for the lowest concentration (0.05 mM L-cysteine), which was close to the detection limit under our experimental conditions. The linear increase to relatively large (5 mM L-cysteine) concentrations is interesting, as there does not seem to be a limitation in available gold surface area. This further suggests that the different cysteine oxidation peak areas for the 5 and 50-nm Au NPs in Fig. 3(b) (threefold bigger area for 5-nm than 50-nm Au NPs) are not necessarily caused by the available surface area but by different cysteine-gold interactions.

In all, the electrochemical investigations suggest selective cysteine-gold interactions and adsorption of cysteine on the citrate precoated Au NPs. ToF-SIMS was used to further understand these interactions.

### C. ToF-SIMS investigation of gold–cysteine interactions

The $Au_3^-$ (*m/z* 590.90) image of a 5-nm Au NPs-loaded Al foil upon rinse with ultrapure water is shown in Fig. 4(a). The image shows that the Au NPs were successfully deposited on the Al foil. We chose to use $Au_3^-$, rather than $Au^-$ (*m/z* 196.97), to represent gold, because $Au^-$ is interfered by $Al_3H_4O_7^-$ (*m/z* 196.94), an ion associated with the Al foil.

For the 5-nm Au NPs-loaded Al foil immersed in the L-cysteine solution followed by drying (no rinse with ultrapure water), as shown in Fig. 4(b), there were much weaker $Au_3^-$ signals. Corresponding images [Figs. 4(c) and 4(d)] show the dehydrogenated molecular and dimer cysteine ion images, i.e., $SC_3H_6NO_2^-$ (*m/z* 120.01) and $S_2C_6H_{11}N_2O_4^-$ (*m/z* 239.02), respectively. These ions have a contrast showing much stronger signals in the areas where the $Au_3^-$ signals were absent in Fig. 4(b). Likewise, the hydrogenated molecular and dimer cysteine ion images shown in Figs. 4(e) and 4(f), respectively, $SC_3H_8NO_2^+$ (*m/z* 122.03) and $S_2C_6H_{13}N_2O_4^+$ (*m/z* 241.03), have a similar contrast to those of the dehydrogenated counterparts. Another two characteristic ions for cysteine are $C_2H_6N^+$ (*m/z* 44.05) and $C_3H_6S^+$ (*m/z* 58.99). These results suggest that there were excessive cysteine molecules on the surface of the 5-nm Au NPs-loaded Al foils. Both cysteine and gold need to be detected at the same location in order to access the expected monolayer of cysteine on Au NPs because the probing depth of ToF-SIMS is 1–3 nm, while the cysteine monolayer is less than 1 nm in thickness. This, thus, requires rinsing of the Au NPs-loaded Al foil after the 1-day-immersion in L-cysteine solution.

Images of $Au_3^-$ and $Au_3S^-$ (*m/z* 622.86) are shown in Fig. 5 for the 5-nm Au NPs-loaded Al foil immersed in 5 mM L-cysteine solution for 1 day, followed by rinsing for the removal of excessive cysteine molecules. Aggregates of the 5-nm Au NPs are clearly seen, as evidenced by the $Au_3^-$ image shown in Fig. 5(a). The contrast of $Au_3S^-$ shown in Fig. 5(b) is identical to that of $Au_3^-$ shown in Fig. 5(a). Images of $Au^-$, $AuS^-$, $Au_2^-$, and $Au_2S^-$ had similar contrasts (data not shown) as that of $Au_3^-$. For the extensively studied SAMs of alkanethiols on the Au surface using ToF-SIMS, negative ions $AuM^-$, Au $[M–H]_2^-$, and $Au_2[M–H]^-$ are characteristic to the thiolate, where M represents the molecular formula of the alkanethiol.[20,21,33] These thiolate ions corresponding to the case of cysteine modified Au NPs are $AuSC_3H_7NO_2^-$, $AuS_2C_6H_{12}N_2O_4^-$, and $Au_2SC_3H_6NO_2^-$. Surprisingly, these ions are extremely weak in our case (Fig. S1 in the supplementary material[34]). This observed difference in the molecular thiolate ion fragmentation between alkane thiolate and cysteine thiolate can be tentatively explained by the chemical difference between the two systems, that is, alkyl chains in the alkanethiols versus amino groups ($–NH_2$) in cysteine. It is well-known that amines are characterized by positive ions, which is due to protonation of the amino

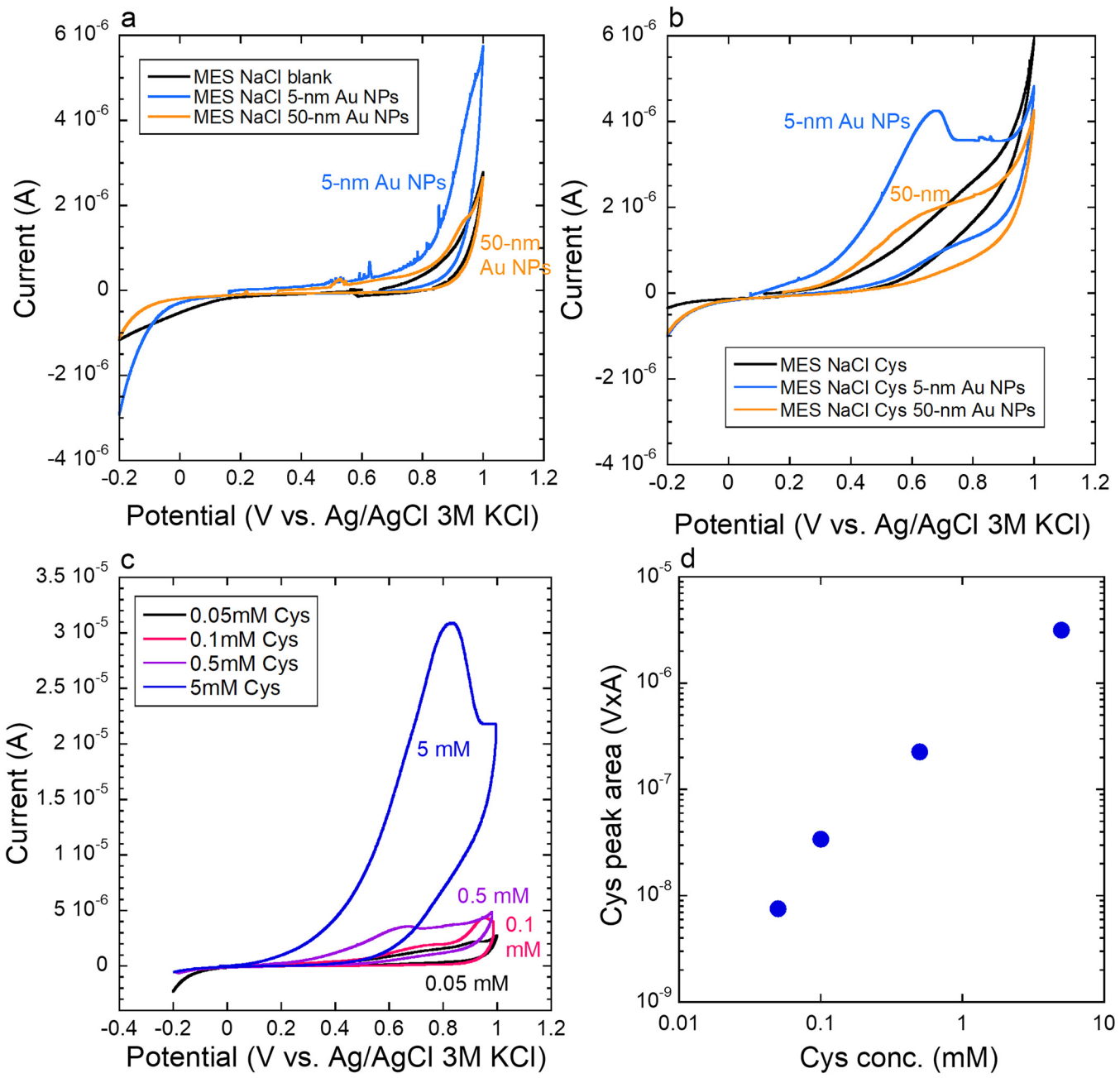


**FIG. 3.** Cyclic voltammograms of the PIGE working electrode in 5 g/l NaCl and 5 mM MES buffer at *p*H 7.4 and room temperature (blank), with $5.56 \times 10^{-4}$ mg 5-nm and 50-nm Au NPs (a), corresponding voltammograms in the presence of 0.5 mM L-cysteine (Cys) (b), and cyclic voltammograms (c) and corresponding cysteine peak area dependence (d) of the PIGE loaded with 5-nm Au NPs in 5 g/l NaCl and 5 mM MES buffer with 0.05, 0.1, 0.5, and 5 mM L-cysteine. Scan rate: 0.5 mV/s; not deaerated; not stirred; conc.—concentration.

group (i.e., the generation of $-NH_3^+$). Therefore, the detection of $Au_xS^-$ can be used as side evidence for the presence of Au–S bonding on the surface of the 5-nm Au NPs that were cysteine-immersed, followed by rinse with ultrapure water.

Figure 5(b) shows the dehydrogenated cysteine molecular ion $SC_3H_6NO_2^-$, showing that the species was associated with the 5-nm Au NPs. Weaker signals outside of the area of the strong $Au_3^-$ signals were due to interference of another species (discussed

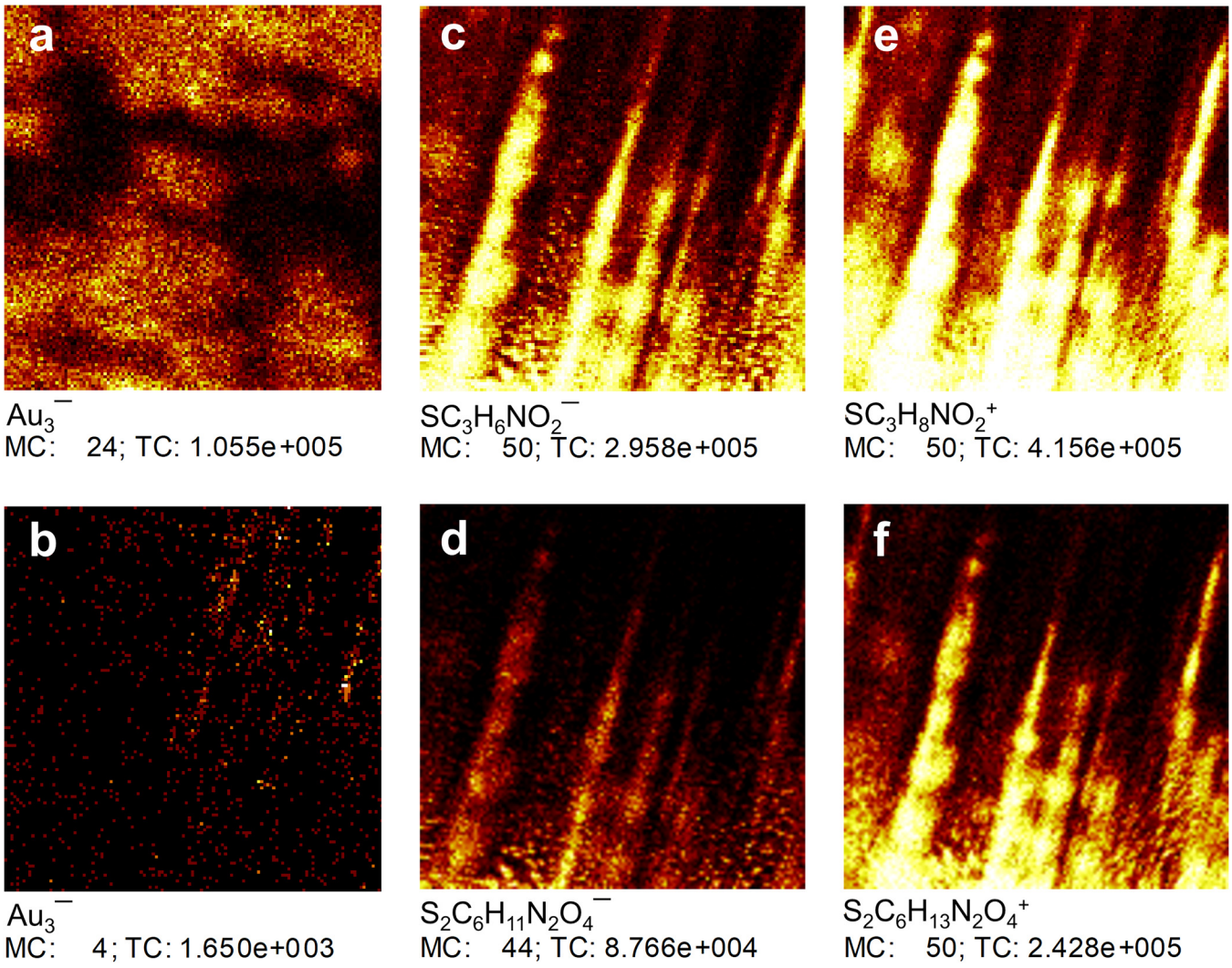


**FIG. 4.** $Au_3^-$ images of (a) the rinsed 5-nm Au NPs-loaded Al foil and (b) the 5 mM L-cysteine solution immersed, 5-nm Au NPs-loaded Al foil (without additional rinsing). Shown in (c) and (d) are corresponding (of b) images of dehydrogenated molecular ($SC_3H_6NO_2^-$) and dimer ($S_2C_6H_{11}N_2O_4^-$) cysteine ions, respectively. The hydrogenated molecular ($SC_3H_8NO^+$) and dimer ($S_2C_6H_{13}N_2O_4^+$) counterparts are shown in (e) and (f), respectively. The rastered areas for (a) and (b)–(f) are 150 × 150 $\mu m^2$ and 500 × 500 $\mu m^2$, respectively. The MC and TC denoted in each image stand for maximum count per pixel and total count over all pixels (128 × 128) for the ion intensity. The ion image is presented in a false color scale, where a brighter color represents a higher ion intensity.

below). As shown in Fig. 5(d), the dehydrogenated cysteine dimer ion $S_2C_6H_{11}N_2O_4^-$ was absent. The experimental observation presented in Figs. 5(c) and 5(d) indicates that cysteine molecules interact with gold to form gold cysteine thiolate so that no free cysteine is available for the formation of cysteine dimers.

The negative secondary ion spectra involving the dehydrogenated cysteine molecular ion $SC_3H_6NO_2^-$ is shown in Fig. S2 in the supplementary material.[34] Figure S2a in the supplementary material is isolated from the areas showing higher $Au_3^-$ and $SC_3H_6NO_2^-$ intensities, while Fig. S2b in the supplementary material is from the entire rastered area. The peak at *m/z* 120.01 in Fig. S2b in the supplementary material is clearly convoluted by at least two peaks, one being $SC_3H_6NO_2^-$. The peak area included by the two blue lines is used to map $SC_3H_6NO_2^-$ [i.e., Fig. 5(c)]. Therefore, though the other peak or peaks could not be identified, they are the contributors to signals mapped in Fig. 5(c) that are outside the $Au_3^-$ contrast area.

Negative secondary ion mass spectra for the comparison of 5-nm Au NPs, cysteine and gold cysteine thiolate are shown in Fig. 6. The 5-nm Au NPs (i.e., gold) spectrum was from the rinsed, 5-nm Au NPs-loaded Al foil without any exposure to cysteine solution [Fig. 4(a)]. The cysteine ion mass spectrum in Fig. 6 was

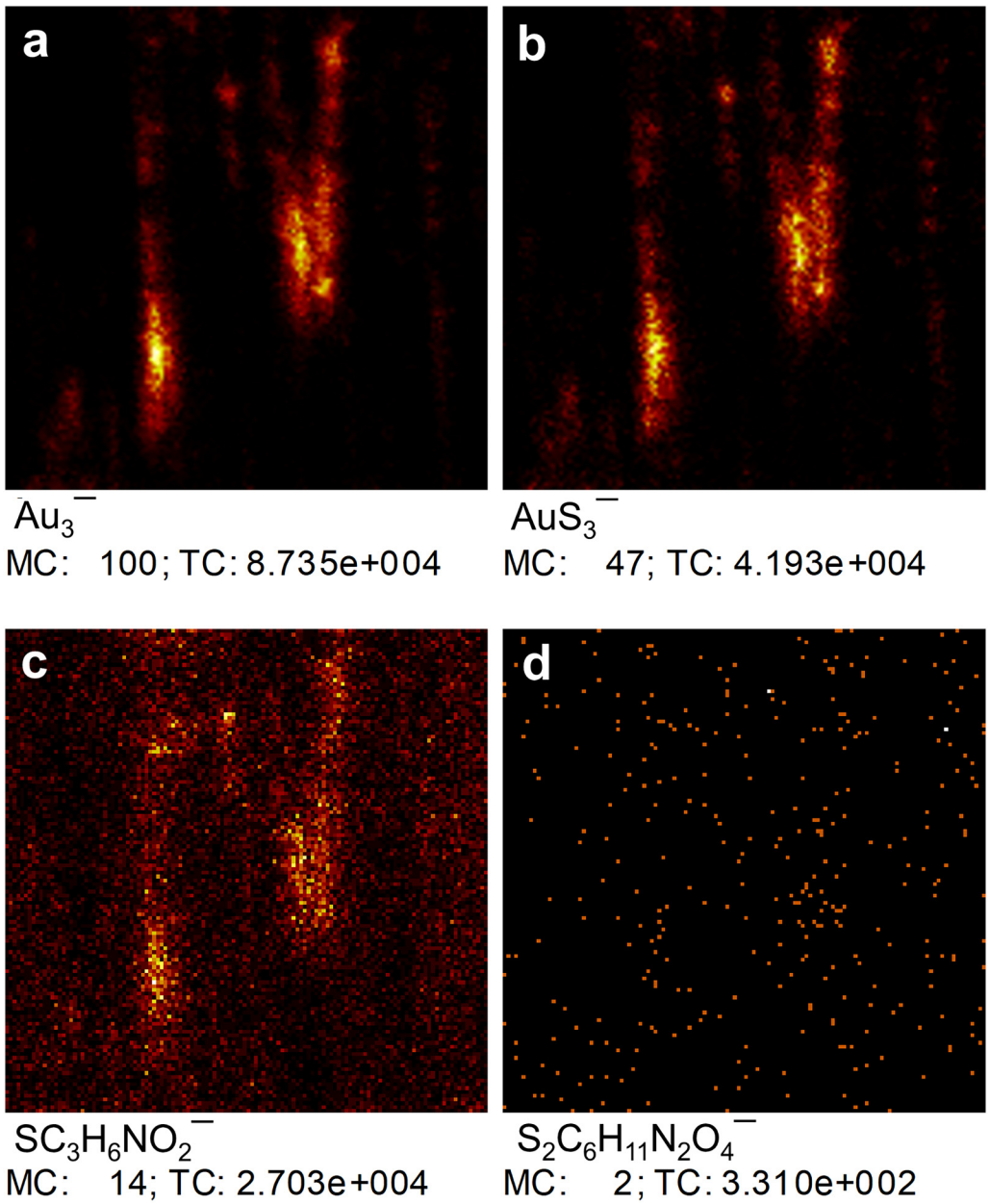


**FIG. 5.** Images of $Au_3^-$ (a), $Au_3S^-$ (b), $SC_3H_6NO_2^-$ (c), and $S_2C_6H_{11}N_2O_4^-$ (d) of the 5-nm Au NPs-loaded Al foil immersed for 1 day in 5 mM L-cysteine solution and rinsed with ultrapure water. The rastered area for (a)–(d) is 244 × 244 $\mu m^2$.

isolated from the cysteine portion of the 5-nm Au NPs-loaded Al foil immersed in the cysteine solution without further rinsing [Fig. 4(c)]. Likewise, the gold cysteine thiolate ion mass spectrum in Fig. 6 was isolated from the gold portion of the rinsed, 5-nm Au NPs-loaded Al foil immersed in the cysteine solution and rinsed with ultrapure water [Fig. 5(a)].

Figure 6(a) shows the $Au_3^-$ and $Au_3S^-$ signals for all these cases. The $Au_3S^-$ signal is weaker than the $Au_3^-$ signal, but present, even in the situation where the 5-nm Au NPs have not been exposed to cysteine, with their intensity ratio being 0.007. This is due to trace-amount sulfur contamination, which, according to our experience, is very commonly seen in ToF-SIMS

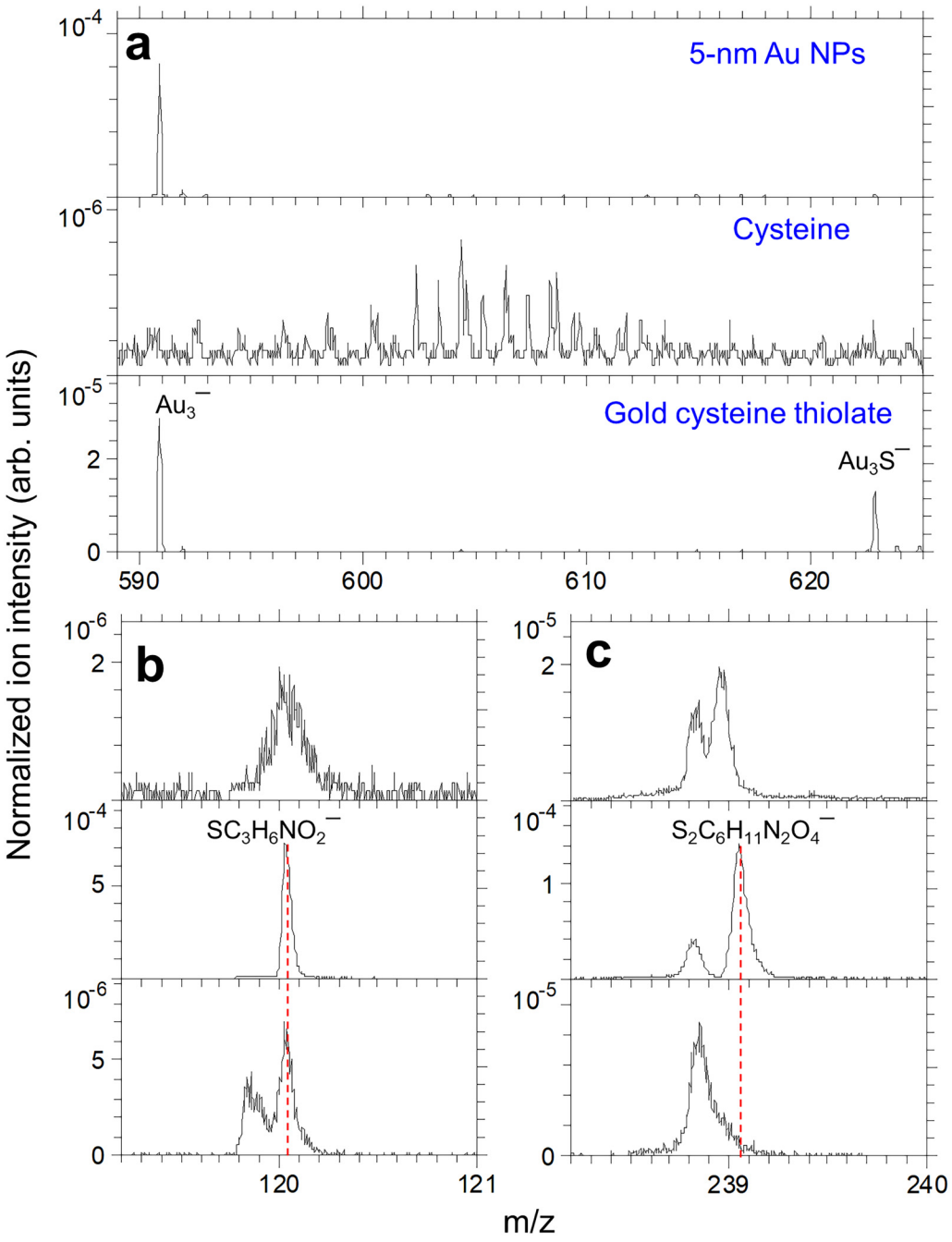


**FIG. 6.** Secondary ion mass spectra representing 5-nm Au NPs (gold) without exposure to cysteine, with exposure to cysteine (without rinsing) and gold cysteine thiolate (after rinsing) showing (a) $Au_3^-$ and $Au_3S^-$, (b) dehydrogenated cysteine molecular ion ($SC_3H_6NO_2^-$), and (c) dehydrogenated cysteine dimer ($S_2C_6H_{11}N_2O_4^-$).

measurements for gold. In contrast, after the 5-nm Au NPs exposure to cysteine solution followed by rinse with ultrapure water, the $Au_3S^-$ to $Au_3^-$ ratio increased to 0.459, an evidence for the Au–S linkage due to binding of cysteine to Au NPs.

The dehydrogenated cysteine molecular and dimer ions, $SC_3H_6NO_2^-$ and $S_2C_6H_{11}N_2O_4^-$, are detected on cysteine, as shown in Figs. 6(b) and 6(c), respectively. However, for the gold cysteine thiolate (i.e., the 5-nm Au NPs exposed to cysteine

solution followed by rinsing), only $SC_3H_6NO_2^-$ is detected, which is explained by the cleaving of the Au–S bond for the formation of gold cysteine thiolate and equivalent to the dehydrogenated cysteine molecular ion. The absence of the dimer shows that cysteine present on Au NPs is no longer a free molecule but covalently bonded to the gold surface. It is still necessary to capture more convincing ToF-SIMS evidence to prove the interaction between gold and cysteine, even though the data in Fig. 6 can serve as side evidence for the formation of gold cysteine thiolate.

Therefore, a careful analysis of positive secondary ion mass images was carried out as well. The important ions mapped in Fig. 7 are a gold cluster ion $Au_3^+$ ($m/z$ 590.90), hydrogenated gold

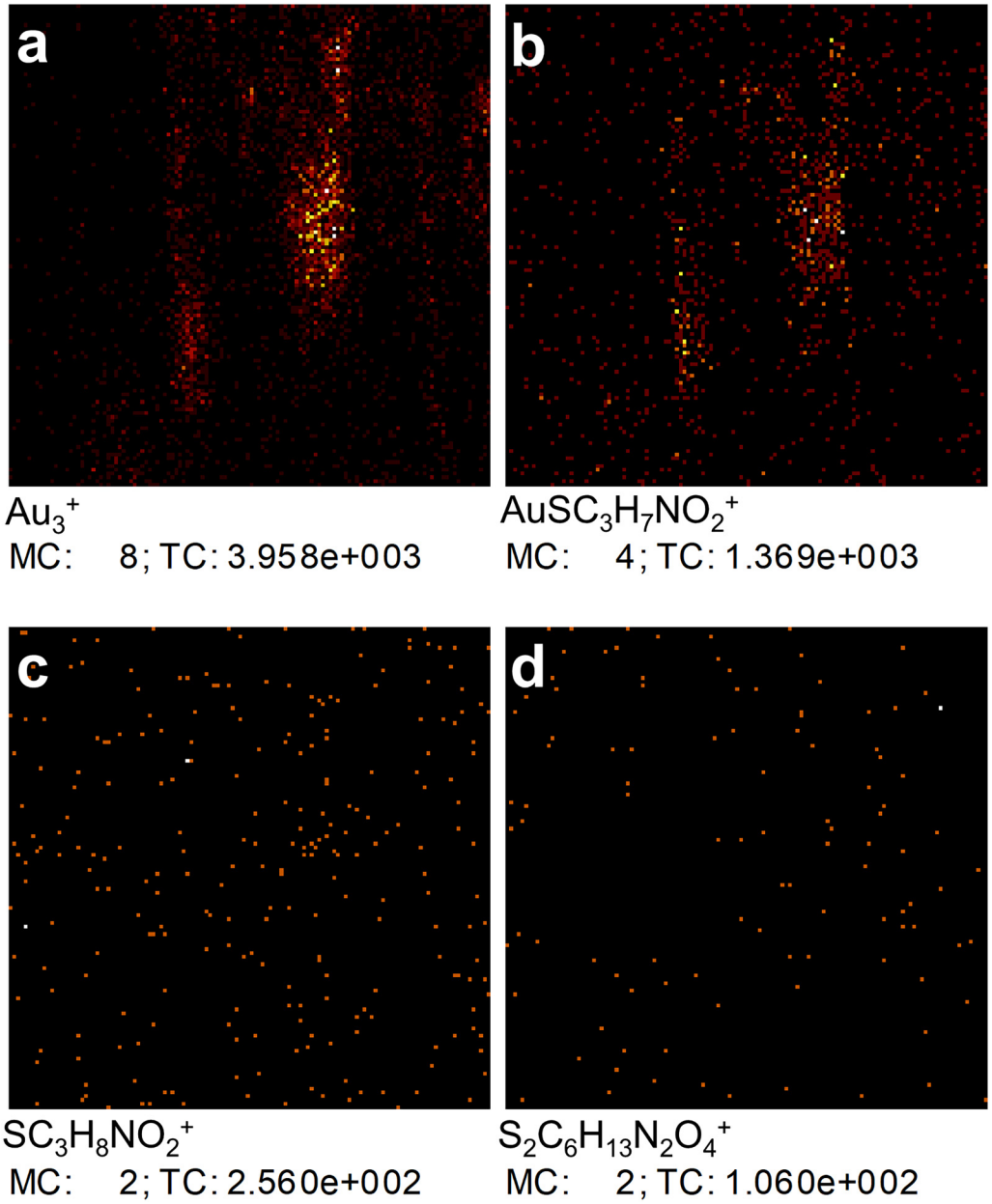


**FIG. 7.** Images of (a) $Au_3^+$, (b) hydrogenated gold cysteine thiolate molecular ion $AuSC_3H_7NO_2^+$, (c) hydrogenated cysteine molecular ion $SC_3H_8NO_2^+$, and (d) hydrogenated cysteine dimer ion $S_2C_6H_{13}N_2O_4^+$ of the 5-nm Au NPs-loaded Al foil immersed for 1 day in 5 mM L-cysteine solution and rinsed with ultrapure water. The rastered area for (a)–(d) is 244 × 244 $\mu m^2$.

cysteine thiolate molecular ion $AuSC_3H_7NO_2^+$ (*m/z* 317.99), hydrogenated cysteine molecular ion $SC_3H_8NO_2^+$ (*m/z* 122.03), and dimer ion $S_2C_6H_{13}N_2O_4^+$ (*m/z* 241.03). The $Au_3^+$ image in Fig. 7(a), with a reduced abundance, is similar to the $Au_3^-$ image shown in Fig. 5(a). Figure 7(b) shows the image of the hydrogenated gold cysteine thiolate molecular ion $AuSC_3H_7NO_2^+$ (*m/z* 317.99), which confirms the interaction between cysteine and gold. Because this ion has never been reported and is most informative for the interaction between cysteine and Au NPs, we carefully examined the ion at *m/z* 317.99 with the help of the known

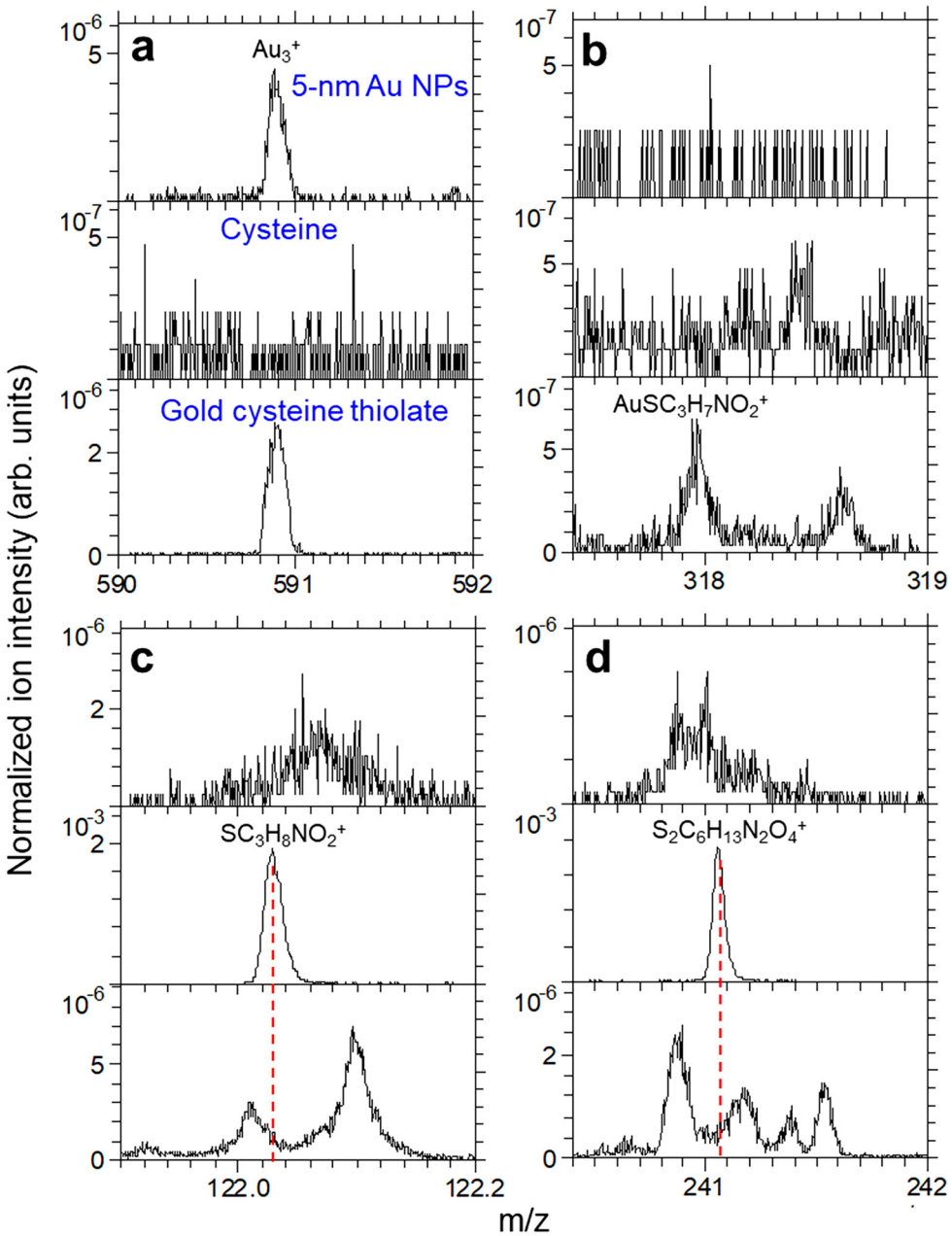


**FIG. 8.** Secondary ion mass spectra representing 5-nm Au NPs (gold) without exposure to cysteine, with exposure to cysteine (without rinsing) and gold cysteine thiolate (after rinsing) showing (a) $Au_3^+$, (b) hydrogenated gold cysteine thiolate molecular ion ($AuSC_3H_7NO_2^+$), (c) hydrogenated cysteine molecular ion ($SC_3H_8NO_2^+$), and (d) hydrogenated cysteine dimer ($S_2C_6H_{13}N_2O_4^+$).

$Au_3^+$. When calibrating the spectrum only with hydrocarbon ions (i.e., $CH_3^+$, $C_4H_7^+$, and $C_6H_9^+$), the deviation for $AuSC_3H_7NO_2^+$ and $Au_3^+$ is −45 and −64 ppm, respectively. Because we are certain about the presence of $Au_3^+$ in the spectrum, we can add it for calibration to cross-check the accuracy of the calibration. When $Au_3^+$ is added for calibration, the deviation for $AuSC_3H_7NO_2^+$ reduces to 4 ppm. This undisputable detection of $AuSC_3H_7NO_2^+$ is readily explained by the emission of gold cysteine thiolate $AuSC_3H_6NO_2$ with the amino group ($–NH_2$) being protonated ($–NH_3^+$).

The detection of this gold cysteine thiolate molecular ion confirms the strong interaction between cysteine and Au NPs, which explains the lack of hydrogenated cysteine molecular ion $SC_3H_8NO_2^+$, as shown in Fig. 7(c), because unlike a free cysteine molecule that requires to capture one hydrogen atom or proton to form $SC_3H_8NO_2^+$, cysteine thiolate would need to capture two hydrogen atoms or protons to form $SC_3H_8NO_2^+$, which is an unlikely event. On the other hand, cleaving the Au–S bond of cysteine thiolate would render dehydrogenated cysteine molecular ion $SC_3H_6NO_2^-$, which explains the detection of the ion shown in Fig. 5(c). The lack of detection of the hydrogenated cysteine dimer ion $S_2C_6H_{13}N_2O_4^+$, as shown in Fig. 7(d), is simply due to the absence of free cysteine molecules.

In fact, Kim *et al.* reported the enhancement of signals of hydrogenated molecular ions of a peptide, $[M + H]^+$, which were adsorbed on Au NPs via $NH_3^+$ groups.[35] This phenomenon can be attributed to the lack of strong bonding between the peptide and the Au NPs. On the other hand, they also reported that for another peptide immobilized on Au NPs via the cysteine sulfhydryl group, they confirmed enhanced signals of $[MH–SH–COOH]^+$ and the lack of $[M + H]^+$.[36] This lack of $[M + H]^+$ signals was a reflection of the strong Au–S linkage between the peptide and Au NPs.[36] In our case, the cysteine equivalent of $[MH–SH–COOH]^+$ is $C_2H_6N^+$, which showed enhanced signals relative to another cysteine ion $C_2H_3S^+$. More specifically, the intensity ratio between $C_2H_6N^+$ and $C_2H_3S^+$ for the cysteine on Au NPs was approximately 10× greater than that for the pure cysteine (Fig. S3 in the supplementary material[34]).

Positive secondary ion mass spectra are shown in Fig. 8 for the 5-nm Au NPs-loaded Al foil (not exposed to cysteine solution), the nonrinsed foil with excess cysteine, and the cysteine-exposed and rinsed 5-nm Au NPs-loaded Al foil, just as in Fig. 6. As shown in Fig. 8(a) (upper panel), gold ($Au_3^+$) signals were detected on Au NPs deposited on the Al foil upon rinse. Figure 8(a) (middle panel) shows that there is no gold detected on the cysteine deposited on the 5-nm Au NPs-loaded Al foil which has been exposed to cysteine solution without subsequent rinsing, suggesting that the Au NPs, if present, are covered by excessive cysteine molecules. After these excessive molecules were removed by rinsing, as shown in Fig. 8(a) (lower panel), gold was detected. As Fig. 8(b) (lower panel) shows, on the cysteine-exposed 5-nm Au NPs, followed by rinse with ultrapure water, the presence of gold cysteine thiolate was confirmed by the detection of hydrogenated gold cysteine thiolate ion, $AuSC_3H_7NO_2^+$. To our best knowledge, this characteristic ion has not been reported in the literature. It is interesting to note that a positive ion $C_{11}H_{26}N_4O_7SAu^+$ was detected[37] on Au NPs functionalized with 1-ß-D-thio-glucose interacted with maltose binding protein solution, suggesting that formation of positive ions involving gold and organic molecules is possible.

As discussed before, gold cysteine thiolate prevents the generation of hydrogenated cysteine molecular ion $SC_3H_8NO_2^+$ [Fig. 8(c)] and dimer ion $S_2C_6H_{13}N_2O_4^+$ [Fig. 8(d)], unlike free cysteine molecules.

We also conducted experiments simulating the environment for the electrochemical interaction between cysteine and Au NPs, which included the MES buffer and sodium chloride, with the solution *p*H adjusted to 7.4 using nitric acid. However, there was no sign of Au NPs detected on the Au NPs-loaded Al foil upon immersion in the solution, rinsed or not. Even when only MES was added in the L-cysteine solution, we still did not detect any gold left on the Al foil. These experimental observations suggest the possibility that MES caused the removal of Au NPs deposited on the Al foil.

To evaluate whether the elaborated ToF-SIMS method could also be used for larger NPs, 50-nm Au NPs were loaded on a clean Al foil and exposed to 5 mM L-cysteine solution for 1 day at room temperature, followed by rinsing with ultrapure water. The resulting negative and positive secondary ion mass images are shown in Fig. S4 in the supplementary material.[34] The 50-nm Au NPs stayed on the Al foil during this procedure and were detected (Figs. S4a, S4b, and S4e in the supplementary material), however, interaction with cysteine, although detected, seemed to be weaker and the positive gold cysteine thiolate signal ($AuSC_3H_7NO_2^+$) was not detected. It remains to be investigated whether the weaker reactions are due to method limitations or weaker interactions of cysteine with larger Au NPs.

The method we used to prepare cysteine covered Au NPs on an Al foil did not allow us to deposit a thicker layer on the substrate. Nevertheless, we were able to have enough cysteine immobilized on Au NPs for ToF-SIMS analysis, which served our purpose. An alternative approach to rendering interactions between Au NPs and cysteine by mixing their solutions followed by dialysis[38] may be worth exploring using ToF-SIMS.

## IV. SUMMARY AND CONCLUSIONS

The aim of this study was to (i) elaborate a ToF-SIMS method able to detect interactions between Au NPs and L-cysteine, (ii) identify the type of these interactions for 5-nm Au NPs, and (iii) evaluate if the method can also be used for the larger-sized 50-nm Au NPs. First, we characterized the size distribution of 5 and 50-nm sized citrate-coated Au NPs, deposited from a suspension on a substrate followed by air-drying. A mean size of 5 and 50 nm was confirmed. Cyclic voltammetry was used to demonstrate selective L-cysteine interaction with the Au NPs. 5-nm Au NPs were more electrochemically active as compared to 50-nm Au NPs in an electrolyte without L-cysteine at *p*H 7.4. In the presence of L-cysteine, the cysteine oxidation peaks were largely magnified by the presence of Au NPs with a threefold larger magnification by the 5-nm Au NPs as compared to the 50-nm Au NPs. This did not seem to be a sole effect of their 100-fold larger specific surface area since the L-cysteine oxidation peaks were linearly increasing with L-cysteine solution concentration, above 0.1 mM L-cysteine, suggesting that the available surface area was not limiting the reaction rate.

ToF-SIMS was used to study the interaction between L-cysteine and Au NPs by depositing the citrate-coated Au NPs from their suspension onto an Al foil followed by immersing the Au NPs-loaded Al foil in a 5 mM L-cysteine solution for 1 day at room temperature. The foil taken out of the solution was covered by excessive cysteine molecules, showing the detection of hydrogenated and dehydrogenated cysteine molecular ions ($SC_3H_8NO_2^+$ and $SC_3H_6NO_2^-$, respectively) and dimer ions ($S_2C_6H_{13}N_2O_4^+$ and $S_2C_6H_{11}N_2O_4^-$, respectively). Rinsing the foil with ultrapure water revealed the formation of gold cysteine thiolate $AuSC_3H_6NO_2$ (in the case of 5-nm Au NPs), as evidenced by the detection and mapping of gold ions (such as $Au^-$, $Au_3^-$, $Au^+$, and $Au_3^+$), dehydrogenated cysteine molecular ion ($SC_3H_6NO_2^-$), ions reflecting thiolate bonds ($AuS^-$ and $Au_3S^-$) and most importantly, hydrogenated gold cysteine thiolate molecular ion ($AuSC_3H_7NO_2^+$). A similar approach in MES buffer and NaCl removed detectable Au NPs from the Al foil, disabling their detection by the ToF-SIMS method. 50-nm Au NPs were possible to detect, with cysteine peaks associated, however, the hydrogenated gold cysteine thiolate molecular ion ($AuSC_3H_7NO_2^+$) was not detectable in their case. Further studies are required to understand the effect of Au NP size on the strength and type of cysteine-gold interactions.

The strengths and limitations of this study are a consequence of the Au NP deposition on substrates: it is possible to use both the electrochemical and the ToF-SIMS methodological approach for small (5-nm) Au NPs and follow their ligand-exchange of the pre-coated citrate ligand with cysteine of higher binding affinity, however, it is unknown which fraction of the Au NPs remains on the substrates and whether they are in direct electrical contact. This might impact relative comparisons of differently sized Au NPs (with different binding affinity to the substrate), resistance, and quantification in the electrochemical measurements.

We demonstrate that the superior chemical selectivity and sensitivity of ToF-SIMS, via detection of elemental and molecular species, provide a unique ability to identify the adsorption of cysteine and formation of gold–cysteine bonds on Au NPs.

## ACKNOWLEDGMENTS

The authors thank the Swedish Research Council (Grant No. 2019-03657), the Swedish Foundation for Strategic Research (Grant No. FFL18-0173), the Swedish Steel Association Jernkontoret (Grant No. Stiftelsen Skandinaviska Malm 6-2020), the Canada Research Chairs Program (Grant No. 950–233099), the European Union Program MOST (Grant No. R-QSUa-65035), and the Ministry of Science and Higher Education of the Russian Federation in the Framework of Increase Competitiveness Program of NUST "MISiS" (Grant No. K2-2020-024) for financial support.

## DATA AVAILABILITY

The data that support the findings of this study are available from the corresponding authors upon reasonable request.

## REFERENCES

[1]D. P. Cormode, P. C. Naha, and Z. A. Fayad, Contrast Media Mol. Imaging **9**, 37 (2014).
[2]C. Peng *et al.*, Angew. Chem. Int. Ed. **58**, 8479 (2019).
[3]X. Huang, I. H. El-Sayed, W. Qian, and M. A. El-Sayed, J. Am. Chem. Soc. **128**, 2115 (2006).
[4]E. C. Dreaden, A. M. Alkilany, X. Huang, C. J. Murphy, and M. A. El-Sayed, Chem. Soc. Rev. **41**, 2740 (2012).
[5]L. Yao, J. Daniels, A. Moshnikova, S. Kuznetsov, A. Ahmed, D. M. Engelman, Y. K. Reshetnyak, and O. A. Andreev, Proc. Natl. Acad. Sci. U.S.A. **110**, 465 (2013).
[6]K. Saha, S. S. Agasti, C. Kim, X. Li, and V. M. Rotello, Chem. Rev. **112**, 2739 (2012).
[7]S. Tang, C. Peng, J. Xu, B. Du, Q. Wang, R. D. Vinluan III, M. Yu, M. J. Kim, and J. Zheng, Angew. Chem. Int. Ed. **55**, 16039 (2016).
[8]A. Heuer-Jungemann *et al.*, Chem. Rev. **119**, 4819 (2019).
[9]U. Carlander, D. Li, O. Jolliet, C. Emond, and G. Johanson, Int. J. Nanomed. **11**, 625 (2016).
[10]U. Carlander, K. Midander, Y. S. Hedberg, G. Johanson, M. Bottai, and H. L. Karlsson, ACS Appl. Bio Mater. **2**, 1006 (2019).
[11]Z. Li, Q. Fu, Y. Xue, and Z. Cui, Mater. Chem. Phys. **214**, 499 (2018).
[12]E. Roduner, Chem. Soc. Rev. **35**, 583 (2006).
[13]S. Lal, R. M. Hall, and J. L. Tipper, Acta Biomater. **42**, 420 (2016).
[14]T. M. Tsao, Y. M. Chen, and M. K. Wang, J. Environ. Monit. **13**, 1156 (2011).
[15]T. A. Larson, P. P. Joshi, and K. Sokolov, ACS Nano **6**, 9182 (2012).
[16]S. Monti, V. Carravetta, and H. Ågren, Nanoscale **8**, 12929 (2016).
[17]L. Caprile *et al.*, Nanoscale **4**, 7727 (2012).
[18]S. Aryal, B. Remant, N. Dharmaraj, N. Bhattarai, C. H. Kim, and H. Y. Kim, Spectrochim. Acta A **63**, 160 (2006).
[19]A. Benninghoven, Angew. Chem. Int. Ed. **33**, 1023 (1994).
[20]M. J. Tarlov and J. G. Newman, Langmuir **8**, 1398 (1992).
[21]D. J. Graham and B. D. Ratner, Langmuir **18**, 5861 (2002).
[22]C. Ghumman, A. Moutinho, A. Santos, A. Tolstogouzov, and O. Teodoro, J. Mass Spectrom. **47**, 547 (2012).
[23]S. Nicolardi, Y. E. Van Der Burgt, J. D. Codée, M. Wuhrer, C. H. Hokke, and F. Chiodo, ACS Nano **11**, 8257 (2017).
[24]J. C. Vickerman and N. Winograd, Int. J. Mass Spectrom. **377**, 568 (2015).
[25]A. M. Belu, M. C. Davies, J. M. Newton, and N. Patel, Anal. Chem. **72**, 5625 (2000).
[26]H.-Y. Nie, Anal. Chem. **82**, 3371 (2010).
[27]C. M. Mahoney, Mass Spectrom. Rev. **29**, 247 (2010).
[28]V. Thiel and P. Sjövall, Annu. Rev. Earth Planet Sci. **39**, 125 (2011).
[29]Y. Cha, Y. Hedberg, N. Mei, and U. Olofsson, Tribol. Lett. **64**, 40 (2016).
[30]B. P. Mainali, D. K. Pattadar, and F. P. Zamborini, J. Electrochem. Soc. **167**, 146503 (2020).
[31]Z. Liu, H. Zhang, S. Hou, and H. Ma, Microchim. Acta **177**, 427 (2012).
[32]Y. Hedberg, M. Norell, P. Linhardt, H. Bergqvist, and I. Odnevall Wallinder, Int. J. Electrochem. Sci. **7**, 11655 (2012).
[33]T. Laiho and J. A. Leiro, Surf. Interface Anal. **40**, 51 (2008).
[34]See the supplementary material at http://dx.doi.org/10.1116/6.0000910 for Figs. S1–S4.
[35]Y.-P. Kim, E. Oh, M.-Y. Hong, D. Lee, M.-K. Han, H. K. Shon, D. W. Moon, H.-S. Kim, and T. G. Lee, Anal. Chem. **78**, 1913 (2006).
[36]Y. P. Kim, E. Oh, Y. H. Oh, D. W. Moon, T. G. Lee, and H. S. Kim, Angew. Chem. **119**, 6940 (2007).
[37]V. Spampinato, M. A. Parracino, R. La Spina, F. Rossi, and G. Ceccone, Front. Chem. **4**, 8 (2016).
[38]R. G. Acres, V. Feyer, N. Tsud, E. Carlino, and K. C. Prince, J. Phys. Chem. C **118**, 10481 (2014).